PERGAMON

Vision Research 42 (2002) 1931–1939

Vision Research

www.elsevier.com/locate/visres

New, sensitive window on abnormal spatial vision: rarebit probing

Lars Frisén *

Department of Ophthalmology, Institute of Clinical Neuroscience, Göteborg University, SE-413 45 Göteborg, Sweden

Received 25 January 2002; received in revised form 2 April 2002

Abstract

Clinical tests have a poor sensitivity to low to moderate degrees of neuro-visual damage, possibly because their test targets involve numerous receptive fields. A new test used briefly exposed microdots of high contrast. Multiple visual field areas were probed repeatedly, with ever-new microdot positions. Normal subjects responded to a median 96.0% of probes. Patients with different visual field defects missed larger numbers of probes within defects and the deeper the defects, the larger the number of misses. Patients with minor chiasmal lesions averaged 1.8 times larger defects in microdot perimetry than in high-pass resolution perimetry, indicating superior sensitivity to minor damage.

Keywords: Spatial vision; Vision loss; Psychophysics; Microdot perimetry

1. Introduction

An important objective of clinical vision tests is to diagnose and monitor disorders causing loss, dysfunction, or disconnection of retinocortical neural channels. Prime examples include glaucoma, compression of the optic chiasm, and cerebral lesions. Most tests approach the objective by varying stimulus characteristics and comparing results with empiric norms. The state of the art is best exemplified by those modern perimeters that involve advanced thresholding strategies, probability density functions, and extensive normative databases (Bengtsson, Olsson, Heijl, & Rootzén, 1997; Johnson & Samuels, 1997). A fundamental question concerns the tests' capacities to reveal early or low-degree neural damage. Theoretical predictions have to await the development of quantitative models. Meanwhile, clinico-pathological and experimental studies using differential light sensitivity (DLS) have revealed that one-quarter to one-half of the retinal output neurons, the ganglion cells, may be lost before perimetry returns abnormal results (Curcio et al., 1993; Harwerth, Carter-Dawson, Shen, Smith, & Crawford, 1999; Kerrigan-Baumrind, Quigley, Pease, Kerrigan, & Mitchell, 2000; Quigley, Dunkelberger, & Green, 1989). Similarly, 20/20 visual acuity (VA) can be upheld with less than two-thirds of the normal number of optic nerve axons (Frisén & Quigley, 1984). There is little indication that other types of tests might perform notably better. This of great concern.

Wanting sensitivity to damage is usually taken to indicate the presence of a reserve capacity or redundancy within the neuro-visual system (e.g., Johnson, 1994; Kerrigan-Baumrind et al., 2000). However, there are plausible alternative or complementary explanations. One relates to the reliance on empirical references for normality. Internal references should produce tighter limits. Another possible explanation for wanting sensitivity relates to the amount of information contained in test targets. Clinical vision tests may well present an excess of information. Importantly, studies employing gratings and optotype letters broken down into elements have shown that a large majority of elements can be removed without degrading normal performance (Geller, Sieving, & Green, 1992; Seiple, Holopigian, Szlyk, & Greenstein, 1995). Similarly, clinical acuity and perimetry targets are large enough to envelop scores of individual receptive fields, which may be overly generous. A new test was devised on these premises.

The information content of test targets was reduced to an extreme by employing briefly exposed microdots. Here, micro refers to resolution limits, and brief refers to tenths of seconds. On these scales, natural eye movements may prevent repeated tests in exactly defined locations, making threshold measurements carry little

* Fax: +46-31-820143.
E-mail address: lars.frisen@neuro.gu.se (L. Frisén).

0042-6989/02/$ - see front matter
PII: S0042-6989(02)00102-5

meaning. Instead, the new test simply probed for the presence of vision at a large number of separate locations, using high contrast. It was anticipated that a normal neural matrix should allow all probes to be seen. With a partial matrix depletion some probes should be seen and some should be missed: the missed proportion should reflect the severity of damage. Additionally, some misses should be expected on physiological grounds, viz., shadowing by retinal vessels (angioscotomata) and normal, age-related losses of retinocortical neural channels (Frisén, 1991; Schiefer et al., 1997).

Dot sizes were set to one-half of average normal minimum angles of resolution. Dots were flashed in ever-new positions within 30 circular test areas of 5° diameter inside 30° of eccentricity. The numbers of dots shown and seen were recorded separately for each test area. In the interest of maximizing information transfer, and so save test time, the test employed pairs of microdots, but in contrast to resolution perimetry, the target components were widely separated (Fig. 1). This made for an easy task and also served to minimize influences from optical faults. The test task was to indicate the number of dots seen (none, one, or two). The use of sparse targets carrying a minimum of information suggested the test name, rarebit perimetry. Subjects included normal controls as well as patients presenting with a variety of common conditions. Being exploratory in nature, this first study did not formally analyse all aspects of test performance.

2. Materials and methods

2.1. Test subjects

Twenty-seven normal controls in the 20–70 years age range were recruited among blood donors and hospital staff. None had any visual complaints. All had normal results in a clinical neuro-ophthalmological examination,

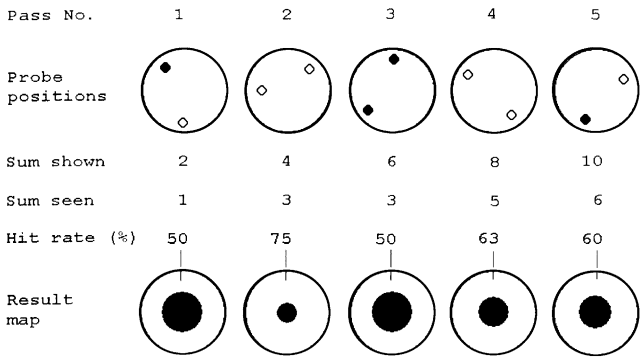

Fig. 1. Schematic representation of rarebit test principle in the presence of a relative visual field defect. From left to right, one and the same circular test area is probed five times, using twin probes (small circles) in ever-new positions. Subject indicates number of probes seen during each presentation (0–2). Not to scale.

including perimetry, usually high-pass resolution perimetry (HighTech Vision, Göteborg, Sweden; ver. 3). HRP is a computer-graphic test employing a novel form of resolution target. It is known to perform at least on par with conventional DLS perimetry. Full details and extensive evaluations have been published (e.g., Chauhan, House, McCormick, & LeBlanc, 1999; Frisén, 1993).

Most control subjects were novices to perimetry. It was arbitrarily decided to test right eyes only, using proper test distance corrections and a comfortable patch over the non-tested eye. Rarebit perimetry was always the last test procedure.

Patients were not included on any statistically representative basis but were selected to exemplify light to moderate degrees of neural damage, as disclosed by routine HRP. Cataract or other defects of the ocular media were grounds for exclusion. Further detail will be provided in later sections.

One exclusion criterion applied to all subjects, viz., ametropia exceeding 3 diopters. All subjects provided informed consent.

2.2. Test setup

Rarebit perimetry depends on standard personal computer (PC) components. A 15″ thin-film transistor, liquid crystal display (LCD) (NEC MultiSync LCD 1525S) produced 0.239-mm square picture elements (pixels) at a frame rate of 60 Hz. Target and background luminances were set to 150 and 1 cd/m^2, respectively (Hagner S-1 Photometer, Solna, Sweden), i.e., similar to those used for acuity charts. Room illumination was approximately 1 lux. A 1-m test distance resulted in a pixel angular subtense of 0.8 min of arc, which is about one-half of the normal minimum angle of resolution at high contrast (2′) at the four central-most test locations (Frisén, 1995; Frisén & Glansholm, 1975; Thibos, Cheney, & Walsh, 1987) (Fig. 2). The more peripheral locations were tested at a 0.5-m distance, scaling targets (by dithering) in accordance with the normal fall-off in resolution (about 6′ at 30°). The very center of the visual field was not included because this would have necessitated a third test distance.

A fixation mark was generated on-screen and moved under PC control to access all 30 test locations in a pseudo-random sequence. The distribution of locations was the same for right and left eyes. 50-mm meniscus-type correcting lenses were used throughout. Any astigmatism was corrected as the spherical equivalent. No headrest was necessary: comfortably seated subjects will sit still enough.

2.3. Test procedure

Thresholding was not used. Instead, repeated probes were made for the mere presence of vision inside a 5°

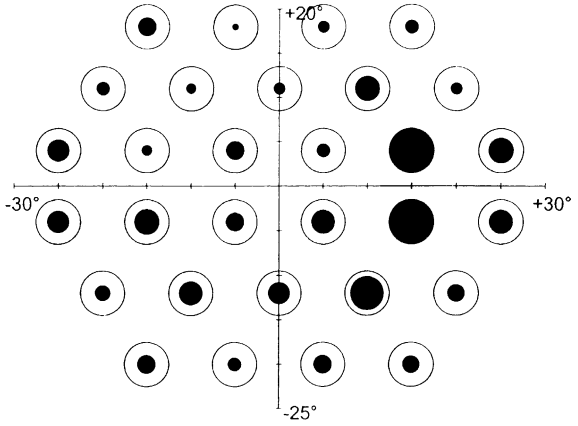

Fig. 2. Size and distribution of test areas in rarebit perimetry. Outer, open circles represent size of test areas. Inner, closed circles represent any missed probes, as the percentage of probes shown (cf. Fig. 1). This diagram does not represent an individual case. Instead, the diagram summarizes the distribution of missed probes over all normal subjects, in right-eye format. For clarity, missed fractions have been multiplied by 10.

diameter circular test area centered on each of the 30 test locations (Fig. 2). Each test presentation contained two microdots exposed simultaneously for 200 ms. Dots were drawn at random positions inside the test area, with the constraint that dot separation must equal 4°. Ten percent of presentations were used for control purposes and contained one dot only, or none at all. The test task was to indicate the number of dots seen during each presentation (0–2), by not clicking, clicking, or double-clicking a mouse button. Dynamic changes of the fixation mark cued in presentation and response intervals and also served to attract and hold attention. The examiner monitored fixation by watching the subject from the side. The test pace was automatically adapted to the current reaction time. Auditory and visual feedback was given.

Following demonstration and a few minutes of training, the first test phase involved one pass over each of the 26 outer locations (Fig. 2). A brief pause was allowed before the next pass. In all, five passes ($=5 \times 2$ microdot presentations at 26 test locations) were made before increasing viewing distance to test the four central-most locations. Five passes were thought to strike a useful compromise between patients' endurance and clinicians' need of detail. Similar considerations lay behind the choices of size and number of test areas.

2.4. Analysis

The test characteristic was the hit rate, i.e., the sum of probes seen divided by the sum of probes shown. Hit rates were plotted separately for each location, using a nested circle format (Figs. 1 and 2). The outer open circle served two purposes. One was to show the size of the test area, the other to scale results. A fully open circle indicated all probes seen (hit rate = 100%). Any missed probes were indicated by adding an inner, filled circle, with proportional diameter (100–hit rate). Hence, a closed circle one-third of the size of the open circle indicated that one-third of the probes presented in this area were not seen. Mean hit rate and standard deviation were calculated over all test locations but the one closest to the blindspot, and for the field quadrants.

2.5. Assessing sensitivity to damage

Sensitivity can be compared relative to another test using a suitable model disorders. It is argued that mid-chiasmal syndromes are nearly ideal model disorders because the associated visual field defects evolve in a predictable pattern. The upper temporal quadrants usually show the most pronounced defects. With increasing damage, the field defects extend first into the lower temporal quadrants, then into the lower nasal ones, and finally into the upper nasal quadrants (Fig. 3). Hence, the typical evolution contains a gradient running around the fixation axis. Individual cases present gradients of different lengths. Gradient length can be expressed as the number of sectors or quadrants scoring outside normal limits (Frisén, 1980). For one and the same individual, different tests may return different numbers, depending on each test's sensitivity to damage: the larger the number, the more sensitive the test. Rarebit perimetry was here compared with HRP, which is known to compare well with conventional DLS perimetry (Dannheim & Roggenbuck, 1989).

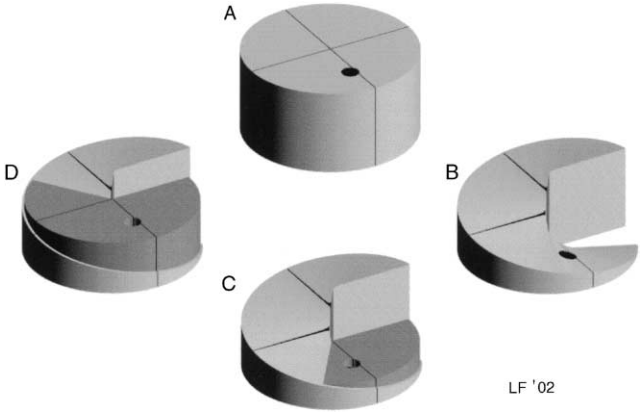

Fig. 3. Model of the range and distribution of visual loss occurring with a mid-chiasmal lesion and results obtained with visual field tests with different sensitivity to damage. (A) Normal right eye central field as seen from lower temporal aspect. Response surface is drawn flat for simplicity. (B) Gradient of field depression, with maximum deficit in upper temporal quadrant. (C) A poor test reflects only a portion of the defect (filled-in sectors). (D) A better test reflects more extensive damage.

3. Results

Initial explorations of the rarebit concept involved larger numbers of dots, forming patterns like digits and simple geometric figures, and more complex response routines. These were all found excessively demanding whereas the current test task—deciding whether none, one, or two dots were seen and clicking correspondingly on a mouse button—proved to be easily mastered and even somewhat entertaining.

The 27 normal subjects obtained a median hit rate of 96.0% (range 88–100), excluding the test location closest to the blindspot. Fig. 2 summarizes the proportion of missed probes (magnified by 10 for clarity) over all normal subjects. Except for the blindspot area, miss rates were fairly uniformly distributed, both in space and magnitude (range 1.5–5.6%). Rates were marginally higher below than above, and still somewhat higher just above and below the blindspot, compatible with minor angioscotoma contributions. In the individual case, one or more misses occurred in a median of eight test locations.

There was a significant effect of age, with hit rates on average decreasing by 1% per decade of age ($r = -0.42$, $p = 0.03$) (Fig. 4). Meanwhile, HRP disclosed a mean change with age of 0.022 dB per year, nearly identical to HRP's reference database, 0.025. HRP automatically performed a number of statistical analyses. No abnormalities were found among the normal subjects and all quality control indices, including fixation, were within normal limits.

True tests of fixation accuracy were not made in rarebit perimetry. Instead, one of the test areas was placed so as to at least partially overlap with the blindspot, with the expectation that good fixation should cause a substantial fraction of probes to be missed in this location. The observed mean percent misses was 79 (median 90, range 30–100).

Control presentations consisted of true blanks or single microdots. The modal number of erroneous responses was 0. Four subjects made four errors or more. Test times averaged 314 s (SD 22), or 63 s per pass, and five passes appeared to be well inside the bounds for sustained attention.

Reproducibility was illustrated by repeated examination of five normal subjects on three different days. Three subjects improved their mean hit rates by 2% or less. Two improved by 4% and 14%, respectively, between the first and second examination, and by 4% and −1% between the second and third. Hence, learning effects were occasionally considerable but were generally small.

Tolerance to optical blur was tested by overcorrecting three normal subjects. +1 diopter had no discernible effect whereas +2 diopters decreased mean hit rate by 10% in the four inner locations in one subject, without affecting the 26 outer ones.

The capability of rarebit perimetry to map a variety of common visual field defects is illustrated in Figs. 5 and 6. These records were selected out of a total of 67 mostly neuro-ophthalmological cases (Table 1), primarily on the grounds of relatively limited neural damage. Figs. 5 and 6 indicate that the fineness of visual field detail obtained with 5° diameter test areas and 30 locations is good enough to describe the spatial distributions and depths of defects, as required for clinical assessment,

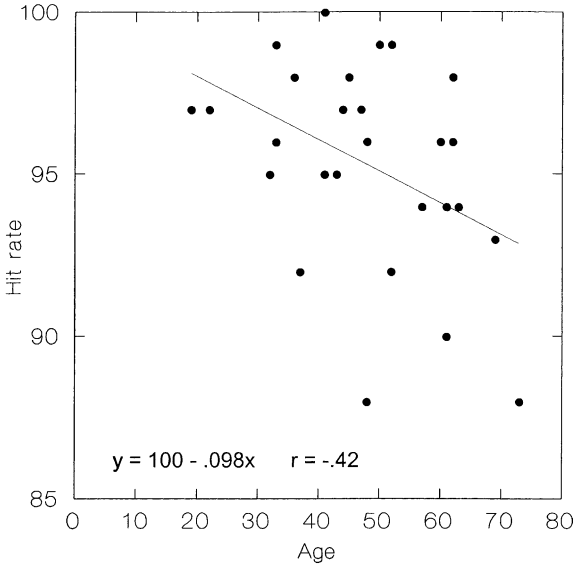

Fig. 4. Mean hit rates of normal subjects as a function of age. Inset: least squares regression parameters and correlation coefficient.

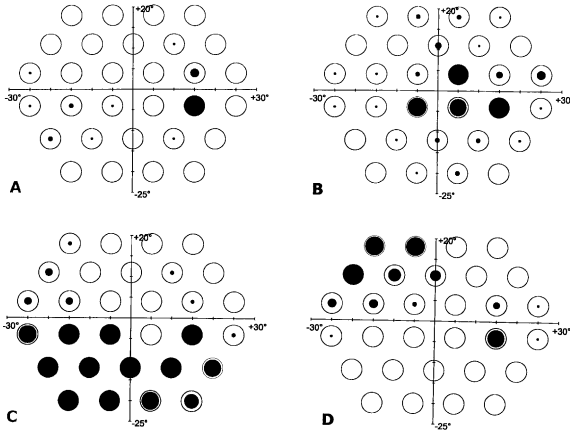

Fig. 5. Examples of focal visual field defects in right-eye format. (A) Subtle lower arcuate scotoma due to chronic papilledema. Mean hit rate 95 ± 2% (SD), decimal VA 1.2. (B) Central scotoma plus scattered smaller defects due to acute demyelinating optic neuropathy. Mean hit rate 79 ± 5%, VA 0.4. (C) Predominantly lower hemifield depression due to non-arteritic anterior ischemic optic neuropathy. Mean hit rate 56 ± 8% VA 0.8. (D) Right-eye component of a homonynous, congruent, upper left quadrant depression, due to first bout of visually asymptomatic MS. Mean hit rate 81 ± 6%, VA 0.8.

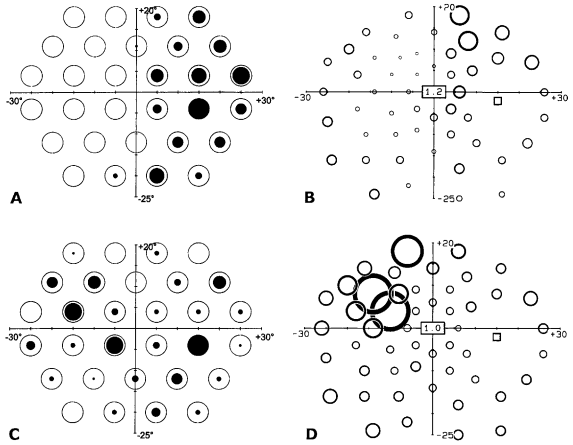

Fig. 6. Examples of rarebit and HRP results from the same right eyes. HRP plots resolution thresholds to scale; nasal hemifield in upper right map exemplifies normal appearance. (A,B) Temporal field depression from mid-chiasmal compression. Mean hit rate $75 \pm 5\%$, VA 1.2. (C,D) Predominantly upper nasal defects from normal-tension glaucoma. Mean hit rate $73 \pm 4\%$, VA 1.0.

Table 1
Summary of diagnoses, numbers of tests, and percent tests outside normal limits (in parentheses)

Diagnosis	Rarebit	HRP
Normal controls	27 (0)	20 (0)
Chronic papilledema	7 (100)	6 (83)
Glaucoma*	7 (43)	7 (29)
Multiple sclerosis	12 (75)	12 (58)
Chiasmal lesion	24 (100)	24 (100)
Various	16 (100)	16 (100)

* Ipsilateral in two instances, contralateral in five.

including differential diagnosis. In all instances, the spatial distributions of defects were similar to those mapped by HRP although the area involved usually was larger.

Relative sensitivity to damage was assessed in 10 patients with light to moderate mid-chiasmal lesions. The diagnosis was verified by magnetic resonance tomography, or surgery, or both. Visual acuities ranged between 0.8 and 1.2 decimal, attesting to low-degree damage. Normal quadrant limits (two standard deviations) were derived from the normal subjects described above. Right-eye results from each of the 10 patients are shown in Fig. 7 as the number of quadrants outside normal limits. Fig. 8 shows raw scores for each quadrant. Plainly, rarebit perimetry disclosed more widespread damage than HRP (3.0 ± 0.82 quadrants involved versus 1.7 ± 0.82, $p = 0.002$). A typical pair of records is shown in Fig. 6A and B. Left-eye results were similar (not shown). It is apparent that rarebit perimetry produced better sensitivity without sacrificing the topographic features required for a topical diagnosis. Expressed in another way, the new test depicted a more advanced stage of disease. Fig. 6C and D exemplify a similar dissociation in a case of glaucoma.

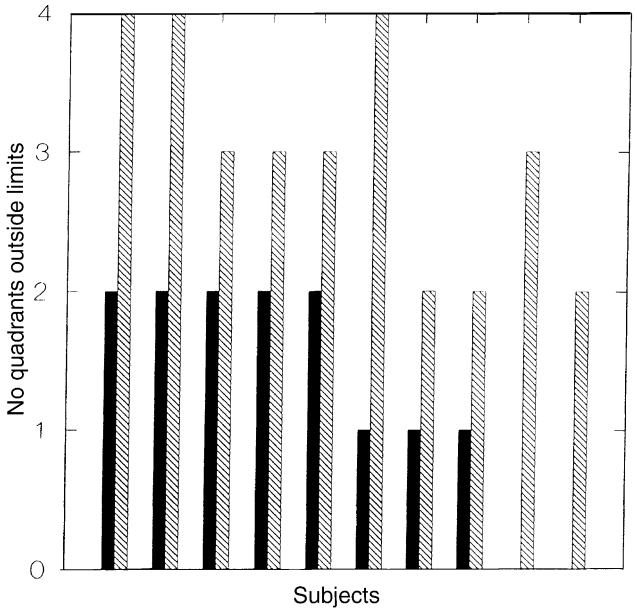

Fig. 7. Number of visual field quadrants outside normal limits in HRP (black bars) and rarebit perimetry (striped bars) in right-eye results from 10 patients with light to moderate mid-chiasmal compression. Subjects have been ordered first on HRP results, then on rarebit. Visual field maps of subject no. 7 are shown in Fig. 6A and B.

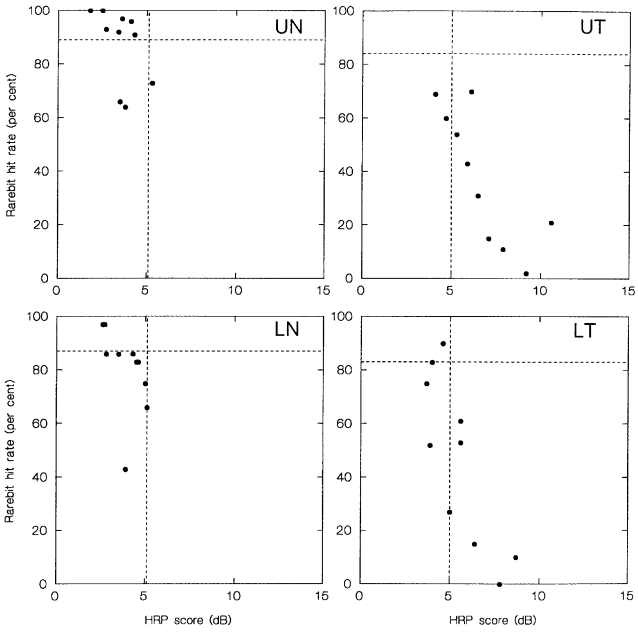

Fig. 8. Distribution by visual field quadrants of raw HRP and rarebit perimetry right-eye scores in 10 subjects with light to moderate chiasmal lesions. Datum points to the right of the dotted vertical lines are outside normal limits in HRP. Datum points below the dotted horizontal lines are outside normal limits in rarebit perimetry. Worst possible score in HRP = 15 dB, in rarebit test = 0%. UT, upper temporal quadrant; LT, lower temporal; LN, lower nasal; UN, upper nasal.

HRP is known to be well accepted by patients. Yet, on informal questioning, a large majority preferred rarebit perimetry. Commonly cited reasons included the more interesting display and the interactive interface.

4. Discussion

The results of this exploratory study indicated that rarebit perimetry was capable of detecting neural damage of various types and degrees. Spatial distributions of defects and defect depths conformed to those expected in ordinary perimetry. Test times, reproducibility, and learning effects were similar. In these respects, rarebit perimetry differs but little from other forms of modern perimetry. The major difference applies to an aspect where the latter are known to fall short, viz., detection of low degrees of damage (Figs. 6–8). The improved detection rate is attributable to two deliberate deviations from standard procedures, viz., minimizing target information content, and replacing thresholding (and its complex statistical overhead) with simple probes of elemental perceptual integrity. Yet, rarebit perimetry is not a stripped down form of conventional perimetry but a new test approach that exploits recent advances in visual physiology and computer graphics. It is dubious whether a practicable implementation of the rarebit concept could have been realized in the recent past.

The following sections will address a number of topics, including optimum test parameters, the question of what is being tested, and limits to detectable damage. Important parameters include target dimensions, in space, in time, and in contrast.

4.1. Target size

Current knowledge of visual system anatomy and physiology does not seem to allow prediction of what microdot size, or more precisely, retinal image size, is optimum for identifying minor neuro-visual damage. Literal point size would be a safe alternative but is difficult or impossible to realize in a clinical setting.

Indications as to maximum allowable microdot sizes might be obtained from two types of existing sources. One is the measurement of the eye's point-spread function (PSF), which provides information on the characteristics of the smallest possible retinal images and their variations with eccentricity (Navarro, Artal, & Willams, 1993; Navarro, Moreno, & Dorronsoro, 1998; Williams, Artal, Navarro, McMahon, & Brainard, 1996). Another source is measurements of psychophysical limits of resolution across the visual field, which provide information on the neural limitations of the eye (e.g., Aubert & Förster, 1857; Frisén, 1995; Frisén & Glansholm, 1975; Thibos et al., 1987). The latter type of measurement has the more direct bearing on the current question. On the other hand, resolution studies have generally employed spatially extended test targets like gratings. Recent reports indicate that extended targets often can be detected at much higher spatial frequencies than those required for resolution. While the percept is unstable and not veridical (Thibos et al., 1987; Williams & Coletta, 1987), the mere phenomenon of so-called aliasing raises the question whether resolution results can directly predict useful microdot sizes. A pragmatic solution is to scale microdots as a fixed fraction of minimum angles of resolution, with the expectation that such scaling should ensure uniform visibility across the visual field. The fraction 0.5 was just within reach of modern computer graphics displays at practicable test distances and so was used here. It appears that refinements of this initial choice may need to be pursued by somewhat unusual means (see further).

Compared with ordinary perimetric test targets, the microdots used here involved literally minuscule visual field areas. For example, the commonly used Goldmann III perimetric target subtends approximately 435 min^2 in object space whereas the microdots subtended no more than 0.7–6.1 min^2 (depending on eccentricity).

4.2. Target generation

The initial explorations of microdot perimetry employed the most common display devices, cathode ray tubes (CRT). Although able to depict moderate and severe degrees of damage, consumer-grade CRTs often failed to reveal low-degree damage, particularly in the central-most test locations. These failures appeared to relate to the size and definition of single picture elements. CRTs tend to produce fairly vaguely delimited pixels. Informal measurements revealed that single white pixels on a dark background usually appeared to be at least twice as large as the screen's nominal resolution, and outside the desired limits. In contrast, LCDs produce crisply defined pixels equal to nominal size. The most common size is 0.3-mm square, which requires minimum 0.5-m test distance (1 m for the paracentral field) to meet the above specifications. Developments in LCD technology tend to produce ever-smaller pixels and higher luminances. A reduction of pixel size by 50%, or more, would allow the use of a single test distance instead of two, as used here. Alternatively, the central-most visual field could be included in the test. Another way to obtain smaller test targets is to use only one out of the three color sub-pixels (red, green, and blue) which together form an achromatic LCD pixel. However, a shift to color seems to require higher luminances than those currently available.

Rarebit targets can be generated in other ways in laboratory settings, e.g., by narrow laser beams, but these generally seem impracticable in clinical work. In-

cidentally, clinical perimeters are not well suited for the task at hand. The smallest standard target, Goldmann Size 0, has a diameter approximating 4′.

4.3. Target luminance and contrast

A high luminance is not necessarily beneficial and may actually be detrimental. Consider the appearance of the stars in the night sky. Although all stars are true point sources, brighter stars are regularly perceived to be larger than fainter stars. This is a reflection of the PSF of the eye, which causes point sources to be imaged with a bright core and tapering flank luminances. It is the level of flank luminances that determine apparent size. These observations clearly have a bearing on optimum luminances of microdot targets, which remain to be explored. It may be that the current choice, which simply aimed to replicate, in reverse, the contrast conditions of clinical acuity tests, was quite fortuitous. Reversed contrast is necessary to maximize image contrast with small detail. Incidentally, the LCDs used in laptop computers are generally unable to produce contrasts of required magnitudes. Further, laptop LCDs often suffer pronounced changes in brightness on small changes in viewing angles.

The use of a dark test background raises the question whether dark adaptation occurs during the test. Because results were stored separately for each 1 min pass, it was possible to search for time-dependent trends, but none were found. This may be attributable to the use of photopic luminance levels for both the fixation mark and the test targets.

4.4. Target timing

Although LCD pixels are well defined geometrically, their temporal properties are not ideal. Essentially depending on electro-chemical processes, LCDs are comparatively sluggish, with response times on the order of 20–40 ms. Hence target exposure times will be long enough to allow eye movements to sweep a number of receptive fields under the target's retinal image. Movements occur in even the most steadily fixating eyes and eye movements are frequently large during clinical perimetry (Henson, Evans, Chauhan, & Lane, 1996). Movements have no detrimental effects on vision in normal eyes (Westheimer & McKee, 1975). However, an eye with a partially depleted neural matrix might benefit from sweeps, even a single sweep as small as a receptive field, if that sweep shifts silent or ailing receptive fields out of the image envelope and shifts a normal receptive field in. Hence, even small sweeps could inflate response rates and cause sensitivity to suffer. From this point of view, it would appear best to aim for exposure times of the order of flashes.

4.5. What is measured?

Normally presenting an essentially flat response surface, rarebit field maps deviate dramatically from the familiar "Hill of Vision" of ordinary perimetry. Further, normal visual fields, which from regular perimetry are known to vary widely both within and between individuals, look much the same in rarebit perimetry. It appears that rarebit perimetry does not measure a gradable quality of vision. Instead, it is submitted that rarebit perimetry tests the integrity of the neural architecture of the visual system. Normally, this architecture is complete in the sense that each and every direction in visual space is continually being monitored for changes in luminance. Completeness of coverage is an inherent system characteristic and by itself irreconcilable with interindividual variation. Although different normal subjects are known to differ with respect to their numbers of retinal ganglion cells and other neural elements (e.g., Curcio & Allen, 1990), and differ in performance in various vision tests, it is submitted that they all share the invariant characteristic of complete coverage. Such a model fits well with the fact that rarebit perimetry normally returns hit rates close to 100% (Figs. 2 and 4). Plausible explanations for the rare non-hits that may occur in normal eyes include angioscotomata, age-related defects in the neural substrate, blinks, and lapses in attention.

Turning to abnormal eyes, most diseases of the neurovisual system are either known or assumed to be associated with architectural defects like loss or disconnection of retinal ganglion cells or their upstream connections. The results of rarebit perimetry indicate that such architectural defects may produce gaps or holes of small angular subtense in the neural matrix, with the production of retinotopically aggregated but essentially sieve-like visual field defects. Further, the spatial density of sieve-like gaps reflects the severity of damage (Figs. 5 and 6).

A sieve-like character of visual field defects may seem to run counter to a century-plus of collected perimetric experience. The difference can in part be understood as a difference in spatial scale. Using test targets enveloping scores of receptive fields, standard tests cannot reflect the finest topographic details of defects. What large targets can reflect is not fully clear: current anatomical and physiological knowledge does not allow prediction of their threshold levels, neither in normal nor in abnormal eyes. In the case of DLS perimetry, a tenuous relationship has been observed between threshold levels and numbers of retinal ganglion cells, but only for moderate and severe levels of damage (Curcio et al., 1993; Harwerth et al., 1999; Kerrigan-Baumrind et al., 2000; Quigley et al., 1989). There may also exist a temporal aspect to the difference between standard and microdot perimetry. The standard approach uses longer exposure times, with

increased risks of overrating function in depleted neural matrices, as outlined above.

4.6. Neural substrate

A much-debated topic of modern perimetry is the targeting of specific channels or classes of retinal ganglion cells. Rarebit perimetry was not specifically designed to meet the tuning properties of any specific ganglion cell class but the small target dimensions might favor the smallest receptive fields. The smallest receptive fields belong to the midget ganglion cells, which project to the parvocellular portion of the lateral geniculate body. These parvocellular channels, which are the most numerous of all channels, are held to mediate resolution (Dacey, 1993; Merigan & Katz, 1990; Wässle & Boycott, 1991). However, experimental inactivation of parvocellular channels does not completely abolish resolution, indicating that other types of channels to a degree may uphold this function (Lynch, Silveira, Perry, & Merigan, 1992). Further, by prohibiting appositioning of fine detail, the rarebit test task differs importantly from resolution tasks. Arguments have been advanced that points, being primitive features of vision, are processed by their own neural mechanism but the anatomical substrate remains elusive (Parker & Newsome, 1998; Westheimer, 1996).

4.7. Detectable damage

A highly relevant question concerns the smallest detectable degree of neural damage. A simple answer relates to the number of probes used per test area. The smallest number of probes that can be missed equals one. For a total of five probes, one miss represents a detectable loss fraction of 0.2, or 20%. The corresponding numbers for 10 probes (as used here) is 10% and for 50 probes 2%. Assuming a spatial uniformity of damage, results may be pooled over several test areas to obtain a higher sensitivity. Such pooling allows recognition of an age-related decline (Fig. 4). Reasoning in terms of numbers of probes only is admittedly very simplistic. More refined modelling requires a probabilistic basis and complex assumptions concerning, i.a., optical imagery, retinal architecture, distributed neural processing, and perceptual mechanisms.

The question whether the rarebit approach can be improved to uncover even smaller degrees of damage than those reported here remains to be studied. The answer has to be sought in a perhaps paradoxical manner, namely, in patients with low-degree visual field defects or field defects with sloping borders. Normal subjects cannot inform on optimum conditions for revealing sieve-like gaps because normal subjects should lack such gaps. However, the study of effects of age-related losses in the neural substrate may form a useful exception (Frisén, 1991).

4.8. Potential applications

Although several questions remain to be answered, the results of this first exploratory study point towards some rather useful roles for rarebit perimetry. Uncovering neuro-visual damage of low degrees may be the most important one. Perhaps paradoxically, the test may also serve the opposite clinical need, i.e., that of a quick check-up, requiring no more than 1 min of testing time for a first outline of the state of the visual system. Detail can then be added as needed by adding new 1 min passes. Another practical role may be to provide quantitative visual field testing in situations where ordinary perimetry is unavailable or impracticable, e.g., at the bedside and in the field.

References

Aubert, H., & Förster, R. (1857). Beiträge zur Kenntsniss des indirecten Sehens. I. Untersuchung über den Raumsinn der Retina. *Archive führ Ophtalmologie, 3*, 1–37.

Bengtsson, B., Olsson, J., Heijl, A., & Rootzén, H. (1997). A new generation of algorithms for computerized threshold perimetry, SITA. *Acta Ophthalmologica Scandinavica, 75*, 368–375.

Chauhan, B. C., House, P. H., McCormick, T. A., & LeBlanc, R. P. (1999). Comparison of conventional and high-pass resolution perimetry in a prospective study of patients with glaucoma and normal controls. *Archives of Ophthalmology, 117*, 24–33.

Curcio, C. A., & Allen, K. A. (1990). Topography of ganglion cells in human retina. *Journal of Comparative Neurology, 300*, 5–25.

Curcio, C. A., Owsley, C., Skalka, H. W., Peters, G. E., Callahan, M. A., & Long, J. A. (1993). Topography of retinal cells and visual sensitivity in the same human eyes ARVO abstract. *Investigative Ophthalmology & Visual Science, 34*, 777.

Dacey, D. M. (1993). The mosaic of midget ganglion cells in the human retina. *Journal of Neuroscience, 13*, 5334–5355.

Dannheim, F., & Roggenbuck, C. (1989). Comparison of automated conventional and spatial resolution perimetry in chiasmal lesions. In: A. Heijl (Ed.), *Perimetry update 1988/89* (pp. 377–382). Amsterdam: Kugler & Ghedini.

Frisén, L. (1980). The neurology of visual acuity. *Brain, 103*, 639–670.

Frisén, L. (1991). High-pass resolution perimetry and age-related loss of visual pathway neurons. *Acta Ophthalmologica, 69*, 511–515.

Frisén, L. (1993). High-pass resolution perimetry. A clinical review. *Documenta Ophthalmologica, 83*, 1–25.

Frisén, L. (1995). High-pass resolution perimetry: central-field neuroretinal correlates. *Vision Research, 35*, 293–301.

Frisén, L., & Glansholm, A. (1975). Optical and neural resolution in peripheral vision. *Investigative Ophthalmology, 14*, 528–536.

Frisén, L., & Quigley, H. A. (1984). Visual acuity in optic atrophy. A quantitative clinicopathological study. *Graefe's Archive of Clinical and Experimental Ophthalmology, 222*, 71–74.

Geller, A. M., Sieving, P. A., & Green, D. G. (1992). Effect on grating identification of sampling with degenerate arrays. *Journal of the Optical Society of America A, 9*, 472–477.

Harwerth, R. S., Carter-Dawson, L., Shen, F., Smith, E. L., III., & Crawford, M. L. J. (1999). Ganglion cell losses underlying visual field defects from experimental glaucoma. *Investigative Ophthalmology and Visual Science, 40*, 2242–2250.

Henson, D. B., Evans, J., Chauhan, B. C., & Lane, C. (1996). Influence of fixation accuracy on threshold variability in patients with open angle glaucoma. *Investigative Ophthalmology and Visual Science, 37*, 444–450.

Johnson, C. A. (1994). Selective versus nonselective losses in glaucoma. *Journal of Glaucoma, 3*, 32–44.

Johnson, C. A., & Samuels, S. J. (1997). Screening for glaucomatous visual field loss with frequency-doubling perimetry. *Investigative Ophthalmology and Visual Science, 38*, 413–425.

Kerrigan-Baumrind, L. A., Quigley, H. A., Pease, M. E., Kerrigan, D. F., & Mitchell, R. S. (2000). Number of ganglion cells in glaucoma eyes compared with threshold visual field tests in the same persons. *Investigative Ophthalmology and Visual Science, 41*, 741–748.

Lynch, J. J., III., Silveira, L. C., Perry, V. H., & Merigan, W. H. (1992). Visual effects of damage to *P* ganglion cells in macaques. *Visual Neuroscience, 8*, 575–583.

Merigan, W. H., & Katz, L. M. (1990). Spatial resolution across the macaque retina. *Vision Research, 30*, 985–991.

Navarro, R., Artal, P., & Willams, D. R. (1993). Modulation transfer of the human eye as a function of retinal eccentricity. *Journal of the Optical Society of America A, 10*, 201–212.

Navarro, R., Moreno, E., & Dorronsoro, C. (1998). Monochromatic aberrations and point-spread functions of the human eye across the visual field. *Journal of the Optical Society of America A, 15*, 2522–2529.

Parker, A. J., & Newsome, W. T. (1998). Sense and the single neuron: probing the physiology of perception. *Annual Review of Neuroscience, 21*, 227–277.

Quigley, H. A., Dunkelberger, G. R., & Green, W. R. (1989). Retinal ganglion cell atrophy correlated with automated perimetry in human eyes with glaucoma. *American Journal of Ophthalmology, 107*, 453–464.

Schiefer, U., Benda, N., Dietrich, T. J., Selig, B., Hofmann, C., & Schiller, J. (1997). Angioscotoma detection with fundus-oriented perimetry. A study with dark and bright stimuli of different sizes. *Vision Research, 39*, 1897–1909.

Seiple, W., Holopigian, K., Szlyk, J. P., & Greenstein, V. C. (1995). The effects of random element loss on letter identification: Implications for visual acuity loss in patients with retinitis pigmentosa. *Vision Research, 35*, 2057–2066.

Thibos, L. N., Cheney, F. E., & Walsh, D. J. (1987). Retinal limits to the detection and resolution of gratings. *Journal of the Optical Society of America A, 4*, 1524–1529.

Wässle, H., & Boycott, B. B. (1991). Functional architecture of the mammalian retina. *Physiological Review, 71*, 447–480.

Williams, D. R., Artal, P., Navarro, R., McMahon, M. J., & Brainard, D. H. (1996). Off-axis optical quality and retinal sampling in the human eye. *Vision Research, 36*, 1103–1114.

Williams, D. R., & Coletta, N. J. (1987). Cone spacing and the visual resolution limit. *Journal of the Optical Society of America A, 4*, 1514–1523.

Westheimer, G. (1996). Location and line orientation as distinguishable primitives in spatial vision. *Proceedings of the Royal Society of London B, 263*, 503–508.

Westheimer, G., & McKee, S. P. (1975). Visual acuity in the presence of retinal-image motion. *Journal of the Optical Society of America, 65*, 847–850.